Hindawi
International Journal of Photoenergy
Volume 2018, Article ID 1862597, 6 pages
https://doi.org/10.1155/2018/1862597

Research Article

1D TiO_2 Nanostructures Prepared from Seeds Presenting Tailored TiO_2 Crystalline Phases and Their Photocatalytic Activity for *Escherichia coli* in Water

Julieta Cabrera,[1] Dwight Acosta,[2] Alcides López,[1] Roberto J. Candal,[3] Claudia Marchi,[4] Pilar García,[1] Dante Ríos,[1] and Juan M. Rodriguez[1]

[1]*Universidad Nacional de Ingeniería, Av. TúpacAmaru s/n, Rimac, Lima, Peru*
[2]*Instituto de Física, Universidad Nacional Autónoma de México, 20364 Ciudad de México, Mexico*
[3]*Instituto de Investigación e Ingeniería Ambiental, CONICET, Universidad Nacional de San Martín, Campus Miguelete, 25 de Mayo y Francia, 1650 San Martín, Provincia de Buenos Aires, Argentina*
[4]*Centro de Microscopias Avanzadas, FCEyN, Universidad de Buenos Aires, Ciudad Universitaria, 1428 Buenos Aires, Argentina*

Correspondence should be addressed to Juan M. Rodriguez; jrodriguez@uni.edu.pe

Received 23 July 2017; Revised 4 December 2017; Accepted 28 December 2017; Published 2 April 2018

Academic Editor: Joaquim Carneiro

TiO_2 nanotubes were synthesized by alkaline hydrothermal treatment of TiO_2 nanoparticles with a controlled proportion of anatase and rutile. Tailoring of TiO_2 phases was achieved by adjusting the pH and type of acid used in the hydrolysis of titanium isopropoxide (first step in the sol-gel synthesis). The anatase proportion in the precursor nanoparticles was in the 3–100% range. Tube-like nanostructures were obtained with an anatase percentage of 18 or higher while flake-like shapes were obtained when rutile was dominant in the seed. After annealing at 400°C for 2 h, a fraction of nanotubes was conserved in all the samples but, depending on the anatase/rutile ratio in the starting material, spherical and rod-shaped structures were also observed. The photocatalytic activity of 1D nanostructures was evaluated by measuring the deactivation of *E. coli* in stirred water in the dark and under UV-A/B irradiation. Results show that in addition to the bactericidal activity of TiO_2 under UV-A illumination, under dark conditions, the decrease in bacteria viability is ascribed to mechanical stress due to stirring.

1. Introduction

TiO_2 nanomaterials are well-studied and commonly used photocatalysts for the degradation of organics, water splitting, and solar cells, among others [1–4]. In the last years, several approaches were explored to increase the photoefficiency of TiO_2, with the modification of the particle morphology and dimensionality being one of the newest [5]. One-dimensional (1D) nanostructures such as nanotubes, nanorods, nanowires, and nanobelts have attracted great attention because of their unique properties that may be beneficial for photocatalysis: (i) enhanced light absorption due to the high length/diameter ratio, (ii) rapid and long-distance electron transport capability, (iii) large specific surface area, and (iv) ion exchange ability [6]. Hydrothermal treatment of TiO_2 particles in alkaline solutions is one of the simplest and cheapest techniques to produce 1D-layered titanate structures. The hydrothermal synthesis of TiO_2 nanotubes involves several steps where the structure of the TiO_2 precursor changes completely.

Results obtained in our laboratories show that 1D TiO_2 nanostructures display photocatalytic activity for dye degradation [7]. Although its performance as a photocatalyst is not as good as other industrially produced TiO_2, this form of TiO_2 can be easily recuperated from the solution.

Furthermore, since 1985 when Matsunaga et al. [8] published the first report of the photocatalytic biocide effects of TiO_2 under metal halide lamp irradiation, there has been increasing interest in photocatalytic disinfection. Use of TiO_2 nanoparticles in suspension is an efficient method for decontamination due to the large surface area of catalysts available to perform the reaction. It has, however, some

drawbacks before its scaling at the industrial level; for example, the necessity of removing the catalyst from the solution after decontamination using filtration increases the cost and time of the cleaning process [9].

In this sense, considering the advantages that our 1D TiO_2 nanostructures are more easily filterable than nanoparticles and can be easily removed from solutions—in addition to the fact that the efficiency of 1D TiO_2 as bactericide under UV-A irradiation was only briefly explored—in this work, we assess the photocatalytic activity of 1D TiO_2, obtained from nanoparticles with a controlled proportion of anatase and rutile made by the sol-gel method, for *E. coli* ATCC 25922 in water.

2. Materials and Methods

2.1. Materials. Titanium isopropoxide purity 98%, hydrochloric acid fuming 37%, nitric acid 65%, and pure sodium hydroxide pellets were purchased from Merck. All reagents were used as received.

2.2. Synthesis of TiO_2 Nanostructures. TiO_2 nanoparticles (TiO_2 NPs) were synthesized by the sol-gel method (SG). Titanium isopropoxide was added drop by drop to vigorously stirred HNO_3 or HCl solutions at pH 0.5, 0.8, and 1.0. Suspensions were heated at 70°C for 2 h, autocleaved in a stainless-steel chamber at 220°C for 12 h, washed by centrifugation, and dried at 60°C.

1D TiO_2 nanostructures were synthesized by hydrothermal treatment of 1 g TiO_2 NPs obtained by the sol-gel method in 40 mL of 10 M NaOH at 130°C for 24 h. After hydrothermal treatment, the obtained white powder was vacuum filtered, washed with HCl solution for ionic exchange, and then washed with distilled water until a neutral pH was reached. Finally, the samples were annealed at 400°C for 2 h to crystallize the material.

The obtained nanostructures were characterized by X-ray diffraction (XRD) in a Rigaku diffractometer using Cu Kα radiation ($\lambda = 1.54056$ Ãƒâ€¦). The morphology was studied by field emission scanning electron microscopy (FE-SEM SUPRA 40, Carl Zeiss) and high-resolution transmission electron microscopy (HRTEM) using a JEOL JEM-2010F transmission electron microscope operating at 200 kV. TEM samples were prepared by dispersing a small amount of the sample in ethanol with the help of an ultrasonic bath. Small droplets of the freshly prepared dispersion were placed onto a copper grid covered with carbon to improve the conduction of the electrons.

2.3. Assessment of Photocatalytic Activity of TiO_2 Nanoparticles and 1D TiO_2 Nanostructures against Escherichia coli in Water. The photocatalytic activity for water disinfection was tested using *E. coli* ATCC 25922. Experiments were performed in a batch reactor, with illumination from above using an Ultra-Vitalux 300 W lamp (30 W/m^2) and, under dark conditions, containing 100 mL aqueous solution with 10^7 CFU/mL bacteria. 1.0 mL aliquots were collected after 0, 20, 40, and 60 min irradiation. Aliquots were diluted 1 : 10 with sterile water to fit in the range 10–500 CFU/mL. 1.0 mL samples of the final dilutions were vacuum filtered through a sterile filter; this results in all bacteria present in the water being retained on the filter. Finally, the filters were placed onto a paper pad soaked in "membrane lauryl sulphate broth" (Oxoid MM0615), which feeds *E. coli* bacteria but inhibits the growth of any other bacteria. The bacterial concentration was determined by counting after 18 h incubation at 37°C.

TiO_2 nanoparticle samples were codified with C or N (for samples made with HCl and HNO_3, resp.) accompanied by 0.5, 0.8, and 1.0, depending on the pH used in the sol-gel synthesis. In a similar way, 1D TiO_2 nanostructures were codified adding 1D to the nanoparticle code (e.g., N0.5 refers to TiO_2 nanoparticles obtained with HNO_3 in pH 0.5, and N0.5-1D refers to a one-dimensional TiO_2 nanostructure obtained for N0.5) resulting in twelve samples.

2.4. Assessment of Stirring in Bacteria Viability. In order to evaluate the mechanical stirring effect in bacteria viability, *E. coli* ATCC 25922 were tested in the dark under stirring (100 rpm) and without stirring at room temperature (20°C). 1.0 mL aliquots were collected after 0, 20, 40, and 60 min stirring.

3. Results and Discussion

3.1. 1D TiO_2 Nanostructures Prepared from Seeds Presenting Tailored TiO_2 Crystalline Phases. Figure 1 shows FE-SEM images of TiO_2 nanoparticles obtained by the sol-gel method (SG-TiO_2 NPs) using HNO_3 and HCl as catalysts in the acid hydrolysis reaction of titanium isopropoxide (pH = 0.5, 0.8, and 1). At pH 1, regardless of the acid, the images show spherical nanoparticles with average diameters of about 15 nm and 13 nm, with HNO_3 and HCl, respectively. Polyhedral structures (60–100 nm) were observed when the pH decreased to 0.8, and octahedral structures with edges of about 140 nm were obtained with HCl at pH 0.5.

XRD patterns (Figures 2(a) and 2(b)) show that the crystalline structures correspond mainly to anatase when acidic solutions with pH 1 were used with both catalysts. Both anatase and rutile were observed with acidic solutions at pH 0.8 and 0.5; a small amount of brookite was detected in most cases. The amount of rutile increased as the pH decreased, and it was the dominant phase when HCl at pH 0.5 was used. The small peak for brookite disappears in this case.

The average crystallite size for anatase and rutile (D_{anatase} and D_{rutile}, resp.), the anatase content, A_p, estimated with the Spurr-Myers equation [10] from the main diffraction peaks, and the pH of the acidic solution (HNO_3 and HCl) are shown in Table 1.

Figure 3 shows the morphology, by FE-SEM, of the 1D nanostructures obtained after alkaline hydrothermal treatment of the sol-gel TiO_2 nanoparticles presented in Figure 1 and Table 1. In the case of SG-TiO_2 synthesized with HNO_3, the particles displayed a tube-like shape, with an average diameter of 11 ± 1 nm in different anatase contents within 18% to 100%, respectively. On the other hand, using as precursor SG-TiO_2 synthesized with HCl acid, flake-like

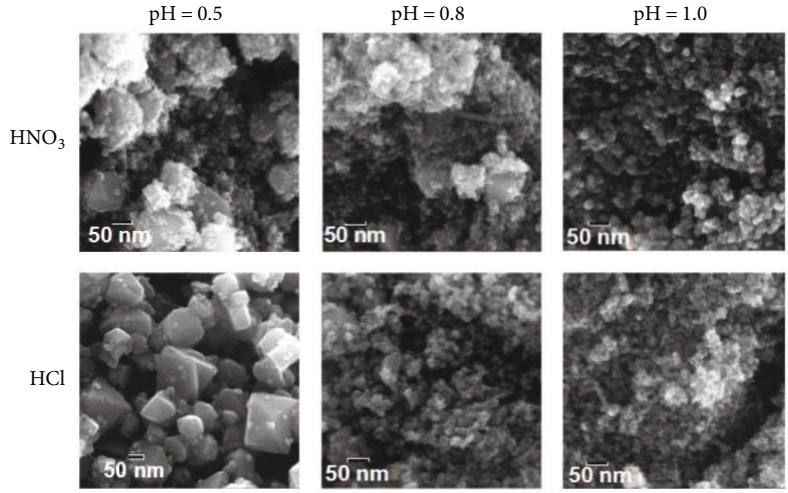

Figure 1: FE-SEM images of TiO_2 nanoparticles obtained from the sol-gel method using HNO_3 and HCl as catalysts of the titanium isopropoxide hydrolysis reaction (pH = 0.5, 0.8, and 1.0, from left to right, resp.).

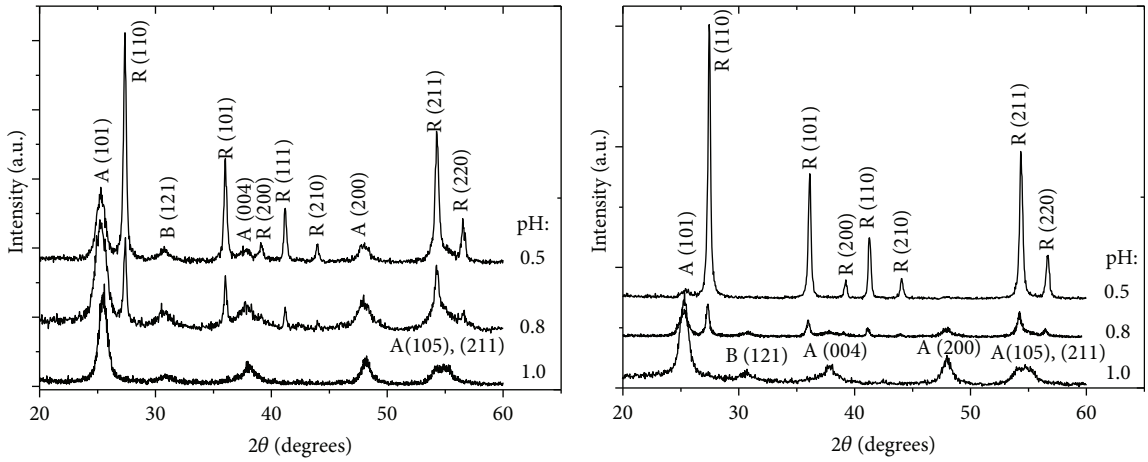

Figure 2: XRD patterns from sol-gel TiO_2 nanoparticles with a range of crystalline phases obtained with (a) HNO_3 and (b) HCl at pH = 0.5, 0.8, and 1.0. (A = anatase; R = rutile; B = brookite).

Table 1: Crystallite size, $D_{anatase}$ or D_{rutile}, and anatase proportion, A_p, of the SG-TiO_2 powders prepared at the indicated pH using HCl or HNO_3 acid solutions.

Catalyst	pH	$D_{anatase}$ (nm)	D_{rutile} (nm)	A_p
	0.5	9.4 ± 0.2	26.8 ± 0.2	0.18
HNO_3	0.8	7.4 ± 0.2	29.0 ± 0.2	0.56
	1	9.0 ± 0.2	—	1
	0.5	—	29.7 ± 0.2	~0.03
HCl	0.8	9.5 ± 0.2	25.9 ± 0.2	0.39
	1	9.8 ± 0.2	—	1

particles were identified together with tube-like structures. The proportion of flake-shaped particles increased as the pH decreased.

After the annealing process at 400°C for 2 h, TEM images (Figure 4) show nanotube structures in all the samples; depending on the seed material, some spherical and rod-shaped structures were also present. It can be seen that a sintering-like process took place during the annealing and that, as a consequence, bundles of tube-like structures and cracked structures were produced.

Tube-like structures seemed to be best conserved when obtained from TiO_2 nanoparticles with 56% of anatase, synthesized with HNO_3. When seed material with lower anatase content (~18%) was employed, large and irregular particles measuring about 80 nm were accompanying the nanotube structures. These might be rutile seed aggregates that could not react in the hydrothermal treatment because of their large particle size. In contrast, needle-like shapes and nanotubes turning to nanorods were observed when anatase-rutile TiO_2 nanoparticles synthesized with HCl were used

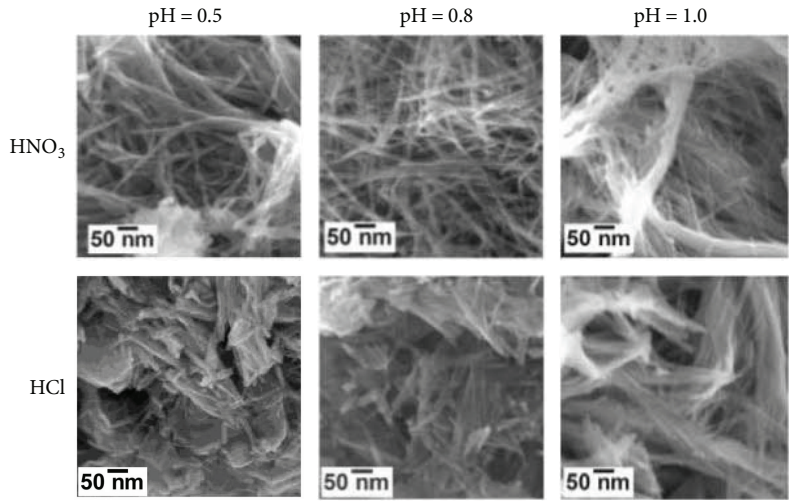

Figure 3: FE-SEM images of 1D TiO_2 nanostructures obtained from SG-TiO_2, prepared with HNO_3 or HCl at pH = 0.5, 0.8, and 1, after 24 h of hydrothermal treatment.

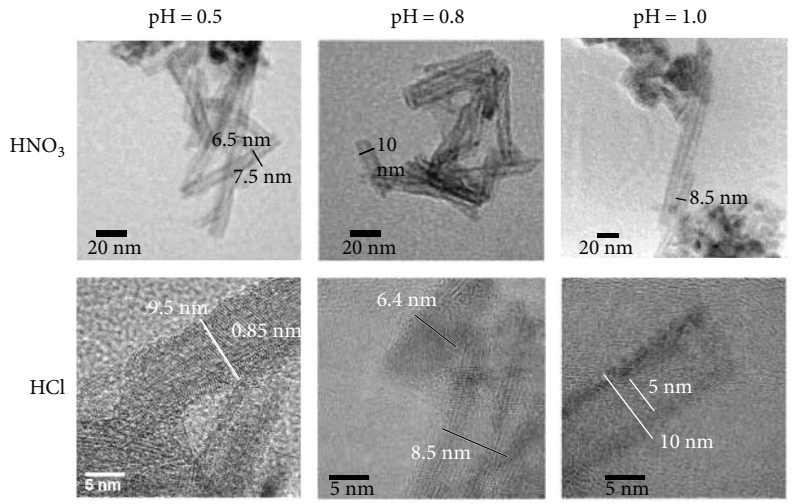

Figure 4: TEM images of 1D TiO_2 nanostructures obtained from SG-TiO_2, prepared with HNO_3 or HCl at pH = 0.5, 0.8, and 1.0, after annealing process (400°C/2 h).

as seed materials. It must be mentioned that, because of the lack of homogeneity in the samples, it is difficult to represent the final TiO_2 structure in a single TEM image; the pictures shown represent the most typical structure in each sample.

The XRD analysis of the samples after hydrothermal treatment (Figure 5(a)) shows that the crystalline structure of the seed material changed and displayed peaks around $2\theta = 10$, 24.5, 28.4, and 48.3°. These peaks represent the diffraction of sodium titanate with the chemical formula $Na_2Ti_nO_{2n+1}$ ($n = 3$, 6, and 9). This is observed for samples where the anatase content in the seed material was higher than 55%. In other cases, rutile was also present as shown by the reflection peaks around $2\theta = 27.5$, 36.1, 41.5, 54, and 56°, corresponding to the (110), (101), (111), (211), and (220) planes in agreement with JCPDS No. 21-1276. This confirms that part of the rutile seeds could remain unreacted after the hydrothermal treatment. After the acid treatment, the features corresponding to titanates almost disappeared, leaving those of the rutile TiO_2 polymorph (not shown).

After the annealing process (Figure 5(b)), a mix of anatase and rutile was observed for samples whose seed had a rutile content larger than 60%. Only peaks corresponding to anatase TiO_2 were observed for samples with anatase higher than 56% in seed. This suggests that when rutile was the dominant phase in the seed material, a portion of it remained unreacted, probably because of the large crystallite size of rutile (~28 nm), compared with the anatase crystallite size (~9 nm). The conditions of the hydrothermal treatment seem insufficient to carry out the dissolution-precipitation process that would be involved in the transformation of TiO_2 to sodium titanate, followed by proton exchange to produce hydrogen titanate and, finally, crystallization to anatase after thermal treatment. On the other hand, it can

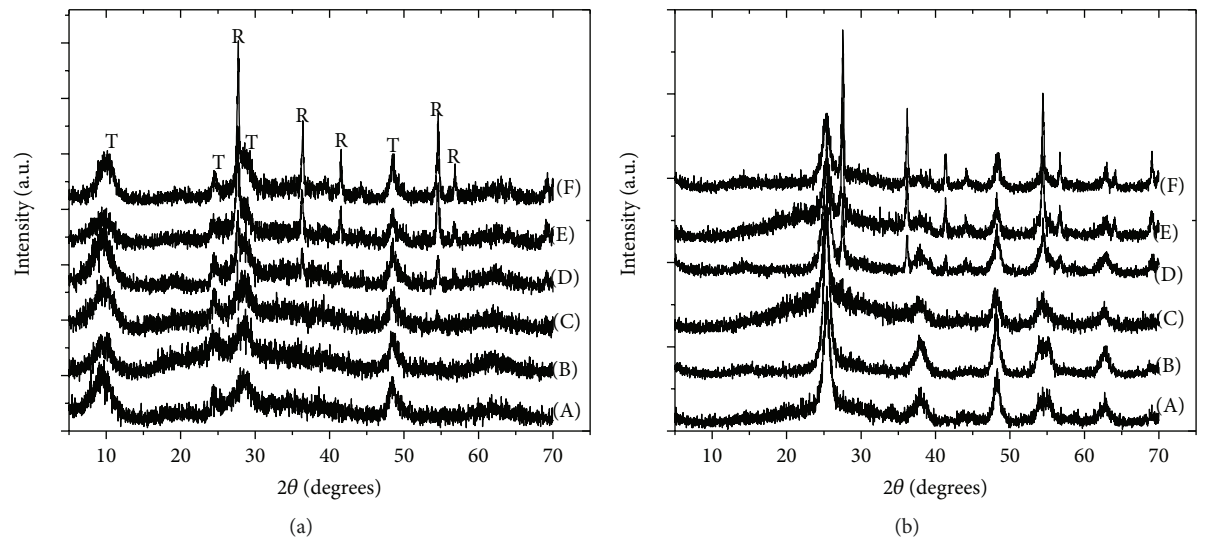

Figure 5: XRD patterns of 1D nanostructures obtained after 24 h of hydrothermal treatment of SG-TiO_2 NPs (a) and the products obtained after the final annealing process at 400°C for 2 h (b). The anatase contents in seeds were (A) ~100% (HNO_3, pH = 1), (B) ~100% (HCl, pH = 1), (C) ~56% (HNO_3, pH = 0.8), (D) ~39% (HCl, pH = 0.8), (E) ~18% (HNO_3, pH = 0.5), and (F) ~3% (HCl, pH = 0.5) (A = anatase; R = rutile).

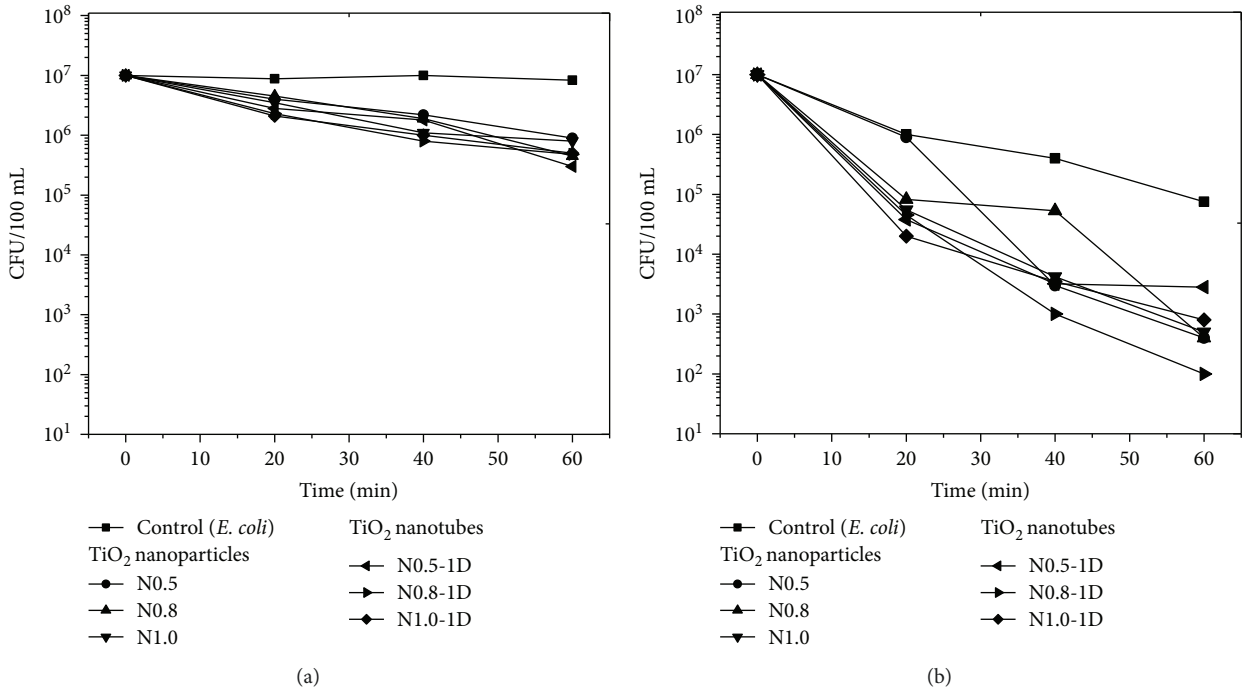

Figure 6: *E. coli* bacteria viability under stirring condition in (a) the dark and (b) under UV-A/B irradiation in the presence of TiO_2 nanoparticles and nanotubes.

be noted that the seed material obtained with HCl produced samples with the best crystallinity, as the X-ray reflections were well defined, compared to those obtained with HNO_3.

3.2. Assessment of the Photocatalytic Activity of TiO_2 Nanostructures for Escherichia coli in Water. Bacteria viability under the stirring process was determined by colony counting after 24 h of incubation. The results showed that the stirring process affects in 1, 3, and 5% (gradually for 20, 40, and 60 minutes, resp.). The assays without stirring were not performed because it was not possible to obtain a homogeneous bacteria distribution.

The effect of stirring in the presence of SG-TiO_2 nanoparticles and their corresponding 1D TiO_2 nanostructures against *E. coli* was evaluated in the dark and under UV-A/B irradiation. As shown in Figure 6, considering that the initial *E. coli* concentration was 1×10^7 CFU/mL, the presence of TiO_2 nanoparticles and nanotubes under stirring

conditions in the dark produced a diminution of bacteria viability of around two orders of magnitude (10^5 CFU/mL). It is ascribed to mechanical stress produced by the stirring process.

Also, as is reported in other studies [11], the photolysis is present in our experiments. It contributes to a decrease in bacteria viability at three orders of magnitude. The bactericidal activity of TiO_2 nanostructures is similar to the photolysis in consequence; the catalyst plus irradiation can decrease bacteria viability until five orders of magnitude. However, no major difference was observed for the bactericidal effect of nanoparticles and one-dimensional TiO_2 nanostructures. The latter have an important advantage since 1D TiO_2 nanostructures can be easily removed from solutions.

4. Conclusions

In summary, TiO_2 anatase 1D nanostructures, with different shapes such as tube- and rod-like shapes, were synthesized by hydrothermal treatment of seeds controlling the anatase-rutile proportion. The synthesized 1D TiO_2 nanostructure was effectively used for photocatalytic abatement of *E. coli* in water. Although the 1D TiO_2 nanostructures have a similar photocatalytic activity than the nanoparticles have, the use of one-dimensional TiO_2 nanostructures has an important advantage since the 1D TiO_2 nanostructure can be easily removed from solutions and could be reusable avoiding the necessity of use filtration that increases the cost and time of the cleaning process.

Conflicts of Interest

The authors declare that they have no conflicts of interest.

Acknowledgments

This work was partially supported by the Innovate Peru Project C.133-PNICP-PIAP-2015 and the Concytec Project 223-2015-FONDECYT-DE. The authors are also grateful to the Microscopy Centre of FCEyN, Universidad de Buenos Aires, and Central Microscopy Laboratory of the Institute of Physics (UNAM). Roberto J. Candal is a member of CONICET.

References

[1] A. J. Cowan, J. Tang, W. Leng, J. R. Durrant, and D. R. Klug, "Water splitting by nanocrystalline TiO_2 in a complete photoelectrochemical cell exhibits efficiencies limited by charge recombination," *The Journal of Physical Chemistry C*, vol. 114, no. 9, pp. 4208–4214, 2010.

[2] D. F. Ollis, E. Pelizzetti, and N. Serpone, "Photocatalyzed destruction of water contaminants," *Environmental Science & Technology*, vol. 25, no. 9, pp. 1522–1529, 1991.

[3] Y. Ren, Z. Liu, F. Pourpoint, A. R. Armstrong, C. P. Grey, and P. G. Bruce, "Nanoparticulate TiO_2(B): an anode for lithium-ion batteries," *Angewandte Chemie International Edition*, vol. 51, no. 9, pp. 2164–2167, 2012.

[4] J. Yan and F. Zhou, "TiO_2 nanotubes: structure optimization for solar cells," *Journal of Materials Chemistry*, vol. 21, no. 26, p. 9406, 2011.

[5] C. W. Lai, J. C. Juan, W. B. Ko, and S. B. A. Hamid, "An overview: recent development of titanium oxide nanotubes as photocatalyst for dye degradation," *International Journal of Photoenergy*, vol. 2014, Article ID 524135, 14 pages, 2014.

[6] N. Liu, X. Chen, J. Zhang, and J. W. Schwank, "A review on TiO_2-based nanotubes synthesized via hydrothermal method: formation mechanism, structure modification, and photocatalytic applications," *Catalysis Today*, vol. 225, pp. 34–51, 2014.

[7] J. Cabrera, H. Alarcón, A. López, R. Candal, D. Acosta, and J. Rodriguez, "Synthesis, characterization and photocatalytic activity of 1D TiO_2 nanostructures," *Water Science & Technology*, vol. 70, no. 6, pp. 972–979, 2014.

[8] T. Matsunaga, R. Tomoda, T. Nakajima, and H. Wake, "Photoelectrochemical sterilization of microbial cells by semiconductor powders," *FEMS Microbiology Letters*, vol. 29, no. 1-2, pp. 211–214, 1985.

[9] S. Ponce, E. Carpio, J. Venero et al., "Titanium dioxide onto polyethylene for water decontamination," *Journal of Advanced Oxidation Technologies*, vol. 12, no. 1, pp. 81–86, 2009.

[10] R. A. Spurr and H. Myers, "Quantitative analysis of anatase-rutile mixtures with an X-ray diffractometer," *Analytical Chemistry*, vol. 29, no. 5, pp. 760–762, 1957.

[11] N. Vermeulen, W. J. Keeler, K. Nandakumar, and K. T. Leung, "The bactericidal effect of ultraviolet and visible light on *Escherichia coli*," *Biotechnology and Bioengineering*, vol. 99, no. 3, pp. 550–556, 2008.